Four-Coloring Model and Frustrated Superfluidity in the Diamond Lattice

Gia-Wei Chern[1] and Congjun Wu[2]
[1]Theoretical Division, Los Alamos National Laboratory, Los Alamos, New Mexico 87545, USA
[2]Department of Physics, University of California, San Diego, California 92093, USA
(Received 17 April 2013; published 15 January 2014)

We propose a novel four-coloring model which describes "frustrated superfluidity" of p-band bosons in the diamond optical lattice. The superfluid phases of the condensate wave functions on the diamond-lattice bonds are mapped to four distinct colors at low temperatures. The fact that a macroscopic number of states satisfy the constraints that four differently colored bonds meet at the same site leads to an extensive degeneracy in the superfluid ground state at the classical level. We demonstrate that the phase of the superfluid wave function as well as the orbital angular momentum correlations exhibit a power-law decay in the degenerate manifold that is described by an emergent magnetostatic theory with three independent flux fields. Our results thus provide a novel example of critical superfluid phase with algebraic order in three dimensions. We further show that quantum fluctuations favor a Néel ordering of orbital angular moments with broken sublattice symmetry through the order-by-disorder mechanism.

DOI: 10.1103/PhysRevLett.112.020601 PACS numbers: 05.50.+q, 03.75.Lm, 67.85.Hj

Strongly frustrated systems are hosts to various complex orders, unusual phases, and elementary excitations. A well-studied example is the emergence of critical Coulomb phases in systems ranging from water ice [1], pyrochlore magnets (spin ice) [2,3] to p-band fermions in the optical diamond lattice (orbital ice) [4]. A common feature shared by these systems is the appearance of an extensively degenerate manifold due to a large number of unconstrained degrees of freedom. Although the macroscopic degeneracy is usually of geometrical origin, especially for magnetic systems [5], the nontrivial spatial dependence of anisotropic orbital interactions in optical lattices provides a new playground for studying interesting phenomena related to a highly degenerate manifold [4,6–8]. In particular, for p-orbital bosonic condensates in optical lattices, the frustrated couplings between the $U(1)$ phase degrees of freedom can lead to intriguing quantum many-body states [9,10].

For conventional superfluid states of bosons, their ground state wave functions are positive-definite as stated by the "no-node" theorem which is valid under very general conditions [11]. It states that the superfluid phases are uniform over the entire condensate, in other words, nonfrustrated. Exotic states of bosons beyond the "no-node" theorem have been theoretically proposed and experimentally realized in ultracold atom optical lattices [12–15]. For example, when bosons are pumped to high orbital bands, their condensate wave functions form nontrivial representations of the lattice symmetry group, dubbed "unconventional" Bose-Einstein condensations, say, the complex-valued $p + ip$-type condensates with spontaneously broken time-reversal symmetry (see Ref. [9] for a brief review). These condensates are metastable excited states, and hence are not constrained by the "no-node" theorem.

In this Letter we study the Bose-Einstein condensates formed by bosons pumped into the p-orbital bands in a diamond optical lattice. We show that the problem of intersite phase coherence in this lattice represents a highly frustrated system and can be mapped to a four-coloring model on the diamond lattice. By combining analytical arguments and numerical simulations, we demonstrate the existence of an algebraic Coulomb phase in the highly degenerate superfluid ground state at the classical level. Our work thus provides a three-dimensional (3D) generalization of the celebrated three-coloring model on the planar honeycomb lattice [16]. Moreover, we also demonstrate a 3D superfluid phase with critical power-law correlations. Finally, we show that quantum order by disorder selects a ground state with an quadrupled unit cell and a Néel ordering of the orbital angular moments.

Model Hamiltonian.—We begin with a discussion of the Hamiltonian for p-orbital bosons in the diamond optical lattice. This bipartite lattice can be generated by the interference of four laser beams with suitably arranged light polarizations as discussed in Ref. [17]. The unit vectors from each site in sublattice A to its four neighboring B sites are denoted as $\hat{\mathbf{n}}_0 = [111]$, $\hat{\mathbf{n}}_1 = [1\bar{1}\,\bar{1}]$, $\hat{\mathbf{n}}_2 = [\bar{1}1\bar{1}]$, and $\hat{\mathbf{n}}_3 = [\bar{1}\,\bar{1}\,1]$. Around the center of each lattice site, the point group symmetry is T_d of which the degenerate $p_{x,y,z}$ orbitals form a triplet irreducible representation. The band energy is thus represented as

$$H_0 = t_\parallel \sum_{\nu=0}^{3} \sum_{\langle ij \rangle \parallel \hat{\mathbf{n}}_\nu} \{ p^\dagger_{i,\nu} p_{j,\nu} + \mathrm{H.c.} \}, \tag{1}$$

where p_ν is the projection of the p orbitals along the direction of $\hat{\mathbf{n}}_\nu$: $p_\nu = \hat{\mathbf{n}}_\nu \cdot \vec{p}$, where $\vec{p} = (p_x, p_y, p_z)$ is a vector of annihilation operators for p orbitals. We only keep the longitudinal hopping between p orbitals along the bond direction, i.e., the σ bonding, and neglect the small transverse hopping terms. Here $t_\parallel$ is positive because of the odd parity of p orbitals [18].

The general on-site interaction has the form $H_{\rm int} = \sum_i V_{ab;cd} p^\dagger_{i,a} p^\dagger_{i,b} p_{i,c} p_{i,d}$, where $V_{ab;cd} = g \int d^3\mathbf{r} \psi_a(\mathbf{r})\psi_b(\mathbf{r})\psi_c(\mathbf{r})\psi_d(\mathbf{r})$, g is the contact interaction parameter, and ψ_a $(a = x, y, z)$ are Wannier functions of p orbitals. The T_d group contains the symmetry of rotation around the z axis followed by the inversion, which transforms $\psi_z \to -\psi_z$, $\psi_x \to -\psi_y$ and $\psi_y \to \psi_x$. Since $V_{ab;cd}$ should be invariant under this transformation, symmetry consideration indicates that there are only two independent parameters $V_{xx;xx}$ and $V_{xy;xy}$. The interaction terms can thus be reorganized as

$$H_{\rm int} = \frac{U}{2}\sum_i \left\{ n_i^2 - \frac{1}{3}L_i^2 \right\} + \Delta U \sum_i \sum_{\alpha=x,y,z} n^2_{i,\alpha}, \quad (2)$$

where $n_{i,\alpha}$ is the particle number in p_α-orbital ($\alpha = x, y, z$) at site $\mathbf{r}_i$, $n_i = n_{i,x} + n_{i,y} + n_{i,z}$, and $L_i^\mu = -\epsilon_{\mu\nu\lambda} p^\dagger_\nu p_\lambda$ is the orbital angular momentum operator. The first term in Eq. (2) represents the Hubbard interaction with the spherical symmetry around the site center and $U = 3V_{xy,xy}$ as given in Refs. [18,9]. We assume repulsive interactions $U > 0$. The ferro-orbital interaction means that bosons prefer to maximize the on-site orbital angular momentum such that their wave functions are most extended spatially to reduce the on-site repulsion [9], analogous to the second Hund's rule of electrons filling in degenerate atomic orbitals. The second term with $\Delta U = \frac{1}{2}(V_{xx;xx} - 3V_{xy,xy})$ comes from the T_d symmetry crystal field. Compared with the spherically symmetric case ($\Delta U = 0$), the angular distributions of Wannier orbitals ψ_a in the diamond lattice expand from $\pm\hat{\mathbf{x}}$, $\pm\hat{\mathbf{y}}$, $\pm\hat{\mathbf{z}}$ toward the the bond directions $\hat{\mathbf{n}}_\nu$. This enhances the interorbital repulsion but weakens the intraorbital one, such that $\Delta U < 0$.

Mapping to the four-coloring model.—We consider the strong coupling case with a weak crystal field $U \gg |\Delta U|$. Assuming that the average filling number per site is large, we approximate each site as a small condensate and treat it classically. The $\Delta U < 0$ term on each site favors a $p + ip$-type on-site condensate, which aligns $\mathbf{L}$ along the cubic directions $\pm\hat{x}$, $\pm\hat{y}$, and $\pm\hat{z}$. In each site the direction of $\mathbf{L}$ is the nodal line of the condensate wave function, around which the $U(1)$ phase winds 2π.

Let us consider site i belonging to sublattice A. The projections of its four bond directions in the xy, yz, and zx planes are evenly distributed. Therefore, no matter which cubic direction $\mathbf{L}_i$ takes, the superfluid phase from site i to its neighbor j along the direction of $\hat{\mathbf{n}}_\nu$ can only be four different values among 0°, 90°, 180°, and 270° up to an overall phase, which is denoted as

$$\varphi_{i,\nu} = \theta_i + \sigma_{i,\nu}\frac{\pi}{2}, \quad (3)$$

where θ_i is the overall phase; $\sigma_{i,\nu} = 0$, 1, 2, and 3 corresponding to colors **R**, **G**, **B**, and **Y**, respectively, in Fig. 1. The phase shift $\theta_i \to \theta_i + \frac{\pi}{2}$ is equivalent to a cyclic permutation among the 4 colors around the direction of $\mathbf{L}_i$; thus, θ_i on each site only takes values from $-\pi/4$ to $\pi/4$. By the same reasoning, the phase from site j on B sublattice to its neighboring site i along the direction of $-\hat{\mathbf{n}}_\nu$ is denoted as $\varphi_{j,\bar{\nu}} = \theta_j + \sigma_{j,\bar{\nu}}(\pi/2)$. The expectation value of the orbital operators appearing in the hopping Hamiltonian (1) is given by $\langle p_{i,\nu}\rangle = +\sqrt{n/3}e^{i\varphi_{i,\nu}}$, and $\langle p_{j,\nu}\rangle = -\sqrt{n/3}e^{i\varphi_{j,\bar{\nu}}}$, for the two respective sublattices, where n is the average filling per site and the quantum depleting of the condensation fraction is neglected. Thus the total kinetic energy summing up all the bonds reads

$$E = -\frac{2}{3}nt_\parallel \sum_{\langle ij\rangle\parallel\hat{\mathbf{n}}_\nu} \cos\left[\theta_i - \theta_j - \frac{\pi}{2}(\sigma_{i,\nu} - \sigma_{j,\bar{\nu}})\right]. \quad (4)$$

To minimize the kinetic energy, we freeze $\theta_i = \theta_j = 0$ for all sites, and match the color on each bond, i.e., $\sigma_{i,\nu} = \sigma_{j,\bar{\nu}} = \sigma_{ij}$. A defect occurs at a bond $\langle ij\rangle$ when $\sigma_{i,\nu} \neq \sigma_{j,\bar{\nu}}$. The defect-free classic ground states of the p-band bosons thus map into a highly frustrated four-coloring model [19]. An example of such configurations in the diamond lattice is shown in Fig. 2. There are $4! = 24$ coloring configurations on each site i, and 6 different orientations $(\pm\hat{\mathbf{x}}, \pm\hat{\mathbf{y}}, \pm\hat{\mathbf{z}})$ for $\mathbf{L}_i$, which are defined as the "chirality" of the condensate. For each chirality, there are $24/6 = 4$ coloring configurations corresponding to a C_4 rotation around the direction of $\mathbf{L}_i$; see Fig. 1. Consequently, the classical ground states correspond to those of the four-coloring model. The chirality can be explicitly computed as $\mathbf{L}_i \| (\hat{\mathbf{n}}_{\pi/2} - \hat{\mathbf{n}}_0) \times (\hat{\mathbf{n}}_\pi - \hat{\mathbf{n}}_{\pi/2})$, where $\hat{\mathbf{n}}_\varphi$ denotes the bond with phase φ at site $\mathbf{r}_i$.

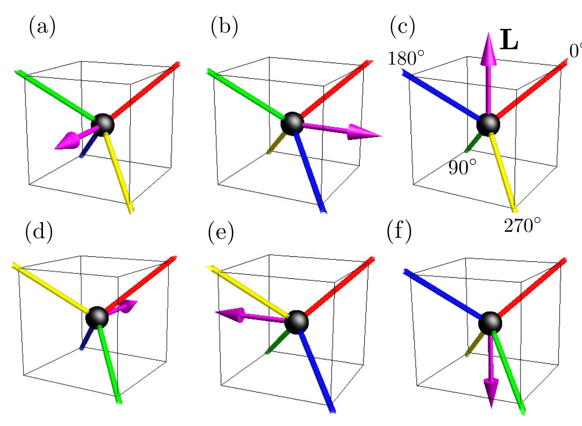

FIG. 1 (color online). Mapping between the orbital angular momentum and color configuration on the diamond lattice. The red, green, blue, and yellow bonds have phases $\phi = 0°, 90°$, 180°, and 270°, respectively, when projected to the base plane perpendicular the direction of angular momentum $\mathbf{L}$. The mapping is not one to one, as each $\mathbf{L}$ corresponds to 4 different cyclic permutations of the colors which preserve the same chirality.

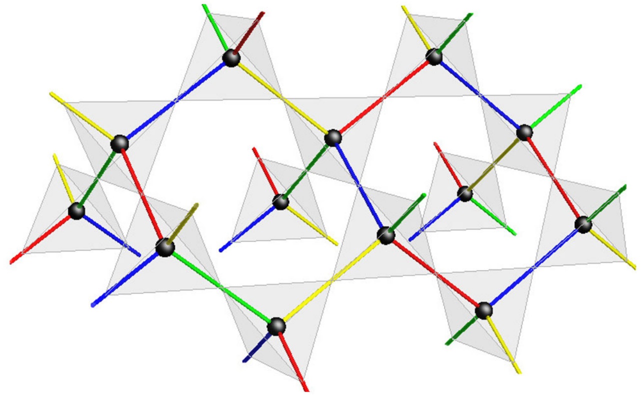

FIG. 2 (color online). An example of valid coloring configuration on the diamond lattice. Here the constraint requires that four bonds attached to the same vertex must have different colors.

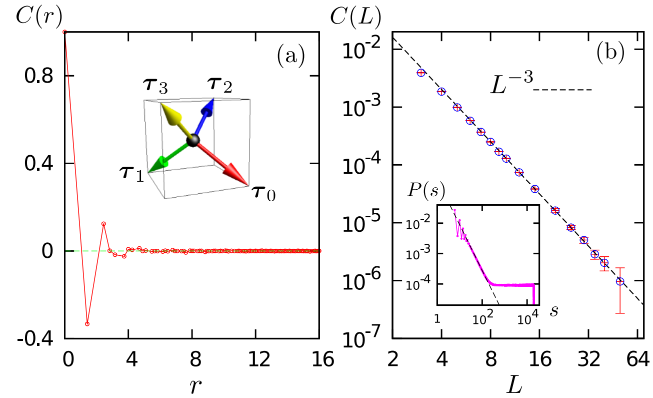

FIG. 3 (color online). (a) The angular averaged superfluidity phase correlation function $C(r) = \langle e^{-i\varphi(r)} e^{i\varphi(0)} \rangle$ on a system with linear size $L = 10$ in the ground state. The inset in (a) shows the four unit vectors $\boldsymbol{\tau}_s$ ($s = 0 \sim 3$) used in the definition of the emergent magnetic fields. (b) Phase correlation vs linear system size L. Here $C(L)$ denotes the color correlation between two points separated by $(L/2, L/2, 0)$ in a finite lattice containing L^3 cubic unit cells. The inset shows the probability distribution $P(s)$ of flippable loop lengths in the critical phase obtained from simulations on a $L = 50$ lattice.

The phase correlation of the p-band condensate has contributions from both the discrete color variables σ_{ij} and the $U(1)$ phases θ_i. At the classic level, it is dominated by the color correlations at low temperatures in which the gapped excitations of defects can be neglected. For all the defect-free configurations, the partition functions for thermal phase fluctuations are identical, and thus the color correlations of σ_{ij} and phase fluctuations of θ_i are decoupled. In 3D, there exists a long-range order for the $U(1)$ phase θ_i below a critical temperature T_c. Consequently, up to a temperature-dependent factor, the correlations of phases $\varphi_{i,\nu}$ are just described by the color correlations.

The residual entropy of the above four-coloring model can be computed using a method similar to the Pauling estimation for the degeneracy of water ice [1]. Consider a given site on the diamond lattice, there is a total of 4^4 different colorings for the four bonds attached to it. Only $4! = 24$ out of the 4^4 coloring schemes satisfy the color constraint. Treating the constraints imposed by different sites as independent, the number of degenerate ground states is $W \sim 4^N (4!/4^4)^{N/2}$, where N is the number of nearest-neighbor bonds and $N/2$ is the number of sites on the diamond lattice. This estimation gives an entropy density: $S_0/k_B = (1/2)\ln(3/2) \approx 0.2027$. Since the four-coloring model on diamond lattice can be mapped to an antiferromagnetic Potts model on pyrochlore with infinite nearest-neighbor couplings (see the Supplemental Material [20]), the residual entropy can also be estimated numerically with the aid of Monte Carlo simulations. The numerically obtained $S_0 \approx 0.2112 k_B$ is very close to the Pauling estimation.

Critical superfluid phase in 3D.—We now investigate the phase correlations of the superfluid wave function in the degenerate manifold. To this end, we employ Monte Carlo simulations with nonlocal loop updates to efficiently navigate the four-coloring manifold [19,21]. In each loop update, two sites are chosen randomly in a given state of the manifold. These two sites will necessarily be of different color, say **R** and **B**. With periodic boundary conditions, a **RB**-colored loop containing the two chosen sites is uniquely determined. By exchanging colors**R** and **B** over the length of the loop, the nonlocal update results in a new state as all the color constraints remain satisfied. Since all the microstates have equal statistical weight, loop updates of all lengths and colors are accepted in order to satisfy detailed balance. The probability distribution of loop length s shown in the inset of Fig. 3(b) exhibits a power-law behavior $P(s) \sim s^{-3/2}$ for short loops, indicating a lack of length scales in the degenerate manifold. The s-independent regime at large loop lengths is due to winding loops in a finite system with periodic boundary conditions [22].

We then employ the above loop-update Monte Carlo simulations to investigate the correlations between the superfluid phases at different bonds: $C(r_{mn}) = \langle e^{-i\varphi_m} e^{i\varphi_n} \rangle$, where $\varphi_m = \varphi_{i,\nu} = \varphi_{j,\bar{\nu}}$, and the bond label $m = \langle ij \rangle$. As discussed above, since the global $U(1)$ symmetry is broken below the critical temperature T_c, the phase fluctuations are mainly governed by the correlations of the color variables σ_m via Eq. (3). By averaging over 10^5 allowed coloring configurations generated by the loop algorithm in a $L = 10$ lattice, we find a phase correlation $C(r)$, shown in Fig. 3(a), that falls off rapidly beyond a few nearest-neighbor distances, indicating a color-disordered phase. Remarkably, the correlation function exhibits a power-law decay $C(L) \sim L^{-3}$ at long distances, as demonstrated in our large-scale Monte Carlo simulations with a number of bonds up to 2×10^6; see Fig. 3(b). This novel state thus provides a rare example of critical superfluid phase with algebraic order in three dimensions. Although this phase is similar to the well-known Kosterlitz-Thouless (KT) phase in 2D, the critical correlations in our case originate from the orbital frustration instead of thermal or quantum fluctuations as in the KT scenario.

Emergent Coulomb phase.—The critical correlations of the p-band superfluid phases can be traced to the nontrivial local ordering imposed by the color constraints. Similar to the case of dimer or spin-ice models [23–26], these local constraints can be mapped to a conservation law of effective magnetic fluxes in the continuum approximation. To this end, we first introduce four unit vectors $\boldsymbol{\tau}_s$ ($s = 0, 1, 2, 3$) pointing toward different corners of a regular tetrahedron [inset of Fig. 3(a)] to represent the four different colorings. We can then construct three "magnetic" fields, each corresponds to a component of the $\boldsymbol{\tau}_s = (\tau_s^x, \tau_s^y, \tau_s^z)$ vectors, at the diamond sites,

$$\mathbf{B}^\alpha(\mathbf{r}_i) = \sum_{\nu=0}^{3} \tau^\alpha_{\sigma_{i,\nu}} \hat{\mathbf{n}}_\nu, \tag{5}$$

where $\alpha = x, y, z$, and $\hat{\mathbf{n}}_\nu$ denotes the nearest-neighbor bond direction. In the coarse-grained approximation, the color constraint that the four color variables $\sigma_{i,\nu}$ around a given site i assume different values translates to a divergence constraint $\nabla \cdot \mathbf{B}^\alpha(\mathbf{r}) = 0$ for the magnetic fields.

The effective free energy of the ground-state manifold arises entirely from entropy and has the form of the magnetostatic theory with three independent flux fields $F[\mathbf{B}^\alpha(\mathbf{r})] \propto \sum_\alpha \int d^3\mathbf{r} |\mathbf{B}^\alpha(\mathbf{r})|^2$. Essentially, it states that the partition function is dominated by microstates characterized by $\mathbf{B}^\alpha \approx 0$. This is due to a large number of flippable loops in such states. Although superficially F describes Gaussian fluctuations of the magnetic fields, the divergence-free constraint in momentum space $\mathbf{k} \cdot \mathbf{B}^\alpha(\mathbf{k}) = 0$ indicates that only transverse fluctuations are allowed. Consequently, the correct correlators are obtained by projecting out the longitudinal fluctuations. The asymptotic field correlators in real space has the famous dipolar form

$$\langle B_a^\alpha(\mathbf{r}) B_b^\beta(0) \rangle \propto \delta_{\alpha\beta}(\delta_{ab} - 3\hat{r}_a \hat{r}_b)/r^3 \tag{6}$$

characteristic of a Coulomb phase [27], which is confirmed in our Monte Carlo simulations; see Fig. 3(d). In terms of the flux fields, the orbital angular momentum can be expressed as $\mathbf{L} \sim \mathbf{B}^\alpha \times \mathbf{B}^\beta$, where the two components $\alpha \neq \beta$ depend on the particular mapping between phases and colors. The correlation function of angular momentum thus exhibits a power-law $1/r^6$ decay in the degenerate manifold.

Four-boson condensate superfluid order.—While the critical phase described above does not have a single-boson long-range superfluid order, there is a four-boson condensate order in this phase as the relative phase differences among $\mathbf{R}$, $\mathbf{G}$, $\mathbf{B}$, and $\mathbf{Y}$ are integer multiples of $2\pi/4$. Contrary to other reports of multiboson superfluid order [28–32] which arises from the interplay of attractive interactions and disordering fluctuations, the four-boson condensate in our case originates from the frustrated intersite phase coherence, i.e., the kinetic energy, which is in turn induced by the anisotropic orbital hopping and geometrical frustration.

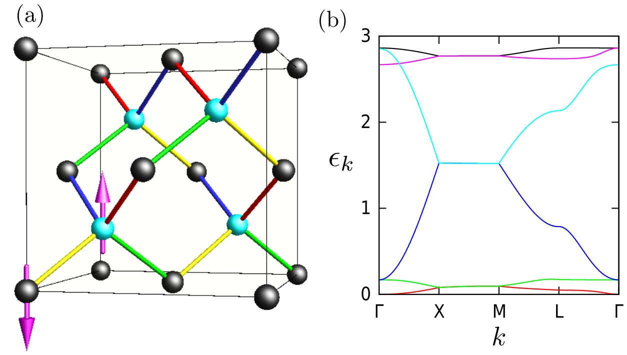

FIG. 4 (color online). (a) Néel ordering of orbital moments $\mathbf{L}$ and the corresponding 4-color configuration. The orbital moments $\mathbf{L}_i$ on the two sublattices (labeled by dark and cyan balls) are antiparallel to each other. (b) shows the band structure of the Bogoliubov quasiparticles in the orbital Néel state ($U/t_\parallel = 0.1$).

Quantum order by disorder.—The extensive classical degeneracy of the four-coloring manifold is removed by quantum fluctuations at the lowest temperatures. Here we consider the effects of zero-point motion energy of elementary excitations in different four-color states. To this end, we first restrict ourselves to long-range orders with a large extended cubic unit cell containing 64 sites. This set of states includes potential orderings with high-symmetry wave vectors such as the K, M, or L points. We then consider fluctuations around the condensate wave function: $\vec{p}_i = \langle \vec{p}_i \rangle + \delta \vec{p}_i$. The quasiparticle spectrum $\epsilon_m(\mathbf{k})$ is then obtained by the standard Bogoliubov analysis [33,34]. By performing simulated annealing simulations to minimize the zero-point motion energy $\frac{1}{2}\sum_{m,\mathbf{k}} \epsilon_m(\mathbf{k})$, we find the state with a staggered arrangement of the orbital moments $\mathbf{L}_i$ shown in Fig. 4(a) is favored by quantum fluctuations.

The band structure of the Bogoliubov quasiparticles in this orbital Néel state is shown in Fig. 4(b). The explicit orbital wave functions on the two sublattices are given by $\langle \vec{p}_{A/B}(\mathbf{r}) \rangle = \frac{1}{2}\sqrt{n}(1, \pm i, 0) e^{i\mathbf{Q}\cdot\mathbf{r}}$ (up to an arbitrary $U(1)$ phase) for the state shown in Fig. 4(a). Here the ordering wave vector $\mathbf{Q} = 2\pi(0, 0, 1)$ and n is the particle density per site. The corresponding orbital moments $\mathbf{L}_{A/B} = \pm n\hat{\mathbf{z}}$ are uniform within the same sublattice (a $\mathbf{q} = 0$ ordering), with the moments of the two sublattices antiparallel to each other.

The long-range ordering induced by quantum fluctuations occurs in both the diagonal and off-diagonal channels, in other words, the (single-boson) superfluid phase ordering and the orbital angular momentum ordering coexist. It is worth noting that since the four-boson off-diagonal order is not due to attractive interaction, there is no threshold (e.g., overcoming a color-disordering gap) for the quantum order-by-disorder mechanism to lift the degeneracy and select the ordered state shown in Fig. 4(a).

Conclusion.—We have studied a diamond-lattice four-coloring model which describes the frustrated couplings between the superfluid phase degrees of freedom for p-band Bose-Einstein condensates in the diamond lattice. We have also shown that the ground states of the four-coloring model are macroscopically degenerate and are described by an effective magnetostatics theory with three independent flux fields. Both color and orbital angular momentum correlations decay algebraically in this emergent Coulomb phase. Interestingly, point defects violating the color constraints carry "magnetic" charges associated with two of the three flux fields. A future direction of study is to explore the kinematics and dynamics of these novel quasiparticles. Finally, we show that the quantum order-by-disorder mechanism lifts the degeneracy and favors Néel ordering of the orbital angular moments.

We are thankful for useful discussions with R. Moessner, Y. Li, and Zi Cai. G. W. C. acknowledges the support of ICAM and NSF Grant No. DMR-0844115. C. W. is supported by Grants No. NSF DMR-1105945 and No. AFOSR FA9550-11-1-0067 (Young Investigator Research Program). C. W. also acknowledges support from the NSF of China under Grant No. 11328403 and the hospitality of the Aspen Center of Physics.

Note added.—Recently, we became aware of similar results on the pyrochlore 4-state Potts model in Ref. [35].

[1] V. F. Petrenko and R. W. Whitworth, *Physics of Ice* (Oxford, New York, 1999).
[2] See S. T. Bramwell and M. J. P. Gingras, Science **294**, 1495 (2001); C. Castelnovo, R. Moessner, and S. L. Sondhi, Annu. Rev. Condens. Matter Phys. **3**, 35 (2012).
[3] N. Shannon, O. Sikora, F. Pollmann, K. Penc, and P. Fulde, Phys. Rev. Lett. **108**, 067204 (2012).
[4] G.-W. Chern and C. Wu, Phys. Rev. E **84**, 061127 (2011).
[5] R. Moessner and A. P. Ramirez, Phys. Today **59**, No. 2, 24 (2006).
[6] C. Wu, Phys. Rev. Lett. **100**, 200406 (2008).
[7] E. Zhao and W. V. Liu, Phys. Rev. Lett. **100**, 160403 (2008).
[8] P. Hauke, E. Zhao, K. Goyal, I. H. Deutsch, W. V. Liu, and M. Lewenstein, Phys. Rev. A **84**, 051603(R) (2011).
[9] C. Wu, Mod. Phys. Lett. A **23**, 1 (2009).
[10] Similar physics has also been studied in Josephson junction arrays of unconventional superconductors, see, e.g. J. E. Moore and D.-H. Lee, Phys. Rev. B **69**, 104511 (2004); C. Xu and J. E. Moore, Nucl. Phys. **B716**, 487 (2005).
[11] R. P. Feynman, *Statistical Mechanics* (Addison-Wesley, Reading, MA, 1972).
[12] A. B. Kuklov, Phys. Rev. Lett. **97**, 110405 (2006).
[13] M. Olschlaeger, G. Wirth, and A. Hemmerich, Phys. Rev. Lett. **106**, 015302 (2011); G. Writh, M. Oelschlaeger, and A. Hemmerich, Nat. Phys. **7**, 147 (2011).
[14] S. Choi and L. Radzihovsky, Phys. Rev. A **84**, 043612 (2011).
[15] X. Li, Z. Zhang, and W. V. Liu, Phys. Rev. Lett. **108**, 175302 (2012).
[16] R. J. Baxter, J. Math. Phys. (N.Y.) **11**, 784 (1970).
[17] O. Toader, T. Y. M. Chan, and S. John, Phys. Rev. Lett. **92**, 043905 (2004).
[18] W. V. Liu, and C. Wu, Phys. Rev. A **74**, 013607 (2006).
[19] J. Kondev and C. L. Henley, Phys. Rev. B **52**, 6628 (1995).
[20] See Supplemental Material at http://link.aps.org/supplemental/10.1103/PhysRevLett.112.020601 for details about the Monte Carlo simulations of the 4-state Potts model on pyrochlore lattice.
[21] D. A. Huse and A. D. Rutenberg, Phys. Rev. B **45**, 7536 (1992).
[22] L. D. C. Jaubert, M. Haque, and R. Moessner, Phys. Rev. Lett. **107**, 177202 (2011).
[23] D. A. Huse, W. Krauth, R. Moessner, and S. L. Sondhi, Phys. Rev. Lett. **91**, 167004 (2003).
[24] S. V. Isakov, K. Gregor, R. Moessner, and S. L. Sondhi, Phys. Rev. Lett. **93**, 167204 (2004).
[25] C. L. Henley, Phys. Rev. B **71**, 014424 (2005).
[26] M. Hermele, M. P. A. Fisher, and L. Balents, Phys. Rev. B **69**, 064404 (2004).
[27] C. L. Henley, Annu. Rev. Condens. Matter Phys. **1**, 179 (2010).
[28] E. Berg, E. Fradkin, and S. A. Kivelson, Nat. Phys. **5**, 830 (2009).
[29] L. Radzihovsky and A. Vishwanath, Phys. Rev. Lett. **103**, 010404 (2009).
[30] F. Zhou, Phys. Rev. Lett. **87**, 080401 (2001).
[31] S. Mukerjee, C. Xu, and J. E. Moore, Phys. Rev. Lett. **97**, 120406 (2006).
[32] C.-M. Jian and H. Zhai, Phys. Rev. B **84**, 060508(R) (2011).
[33] D. van Oosten, P. van der Straten, and H. T. C. Stoof, Phys. Rev. A **63**, 053601 (2001).
[34] Z. Cai, Y. Wang, and C. Wu, Phys. Rev. B **86**, 060517 (2012).
[35] V. Khemani, R. Moessner, S. A. Parameswaran, and S. L. Sondhi, Phys. Rev. B **86**, 054411 (2012).